International Journal of Research in Engineering, Science and Management
Volume 5, Issue 5, May 2022
https://www.ijresm.com | ISSN (Online): 2581-5792

Detection of Glaucoma using Deep Learning

Ravi Kumar Gupta[1], Utkarsh Sharma[2*], Vivek Singh[3]
[1,2,3]Student, Department of Computer Science and Engineering, Meerut Institute of Engineering and Technology, Meerut, India

***Abstract*: Glaucoma is an incurable disease that impairs vision and livability. We used a convolutional neural network to construct a deep learning framework for the identification of spontaneous eye problem in this study. In-depth instructional strategies, like as convolutional neural networks, might evaluate visual sequences in which glaucoma as well as non-glaucoma characteristics may be segregated for testing objectives. The suggested Deep Learning architecture comprise of six study layers: four conv layers and two completely functional levels. Discontinuation and augmentation methods are utilized to increase the accuracy of glaucoma diagnosis. ORIGA and SCES details have been thoroughly tested.**

***Keywords*: area under curve, digital fundus image, region of interest, optic disc, cup disc ratio.**

1. Introduction

Glaucoma is among the causes of visual impairment, affecting an estimated 80 million people by 2021. A chronic eye disorder that gradually damages the visual cortex, resulting in vision loss. Glaucoma is characterised as the "silent robber of vision" as symptoms do not present until the disease has progressed significantly. Glaucoma cannot be cured; however, it can be postponed with medicine. It is vital to diagnose glaucoma promptly utilising high-quality imaging.

Digital fundus imagining is among the most prevalent and extensively utilised ways of detecting glaucoma. DFI has emerged as a popular method for diagnosing major glaucoma because it is possible to detect DFIs in an unusual way that is suitable for major tests. In a glaucoma screening program, the default system determines whether the image has symptoms of glaucoma. Only those images that are considered suspicious in the system will be forwarded to optometrists for further examination. Only images that are considered suspicious by the algorithm will be forwarded to the optometrist for further review. The impairment of optical nerve fibres alters the architecture of the Optic Disc structure, resulting in the enlargement of the cup region (narrowing of the neuro-retinal border), also known as cupping. Because cup enlargement with respect to OD is one of the most common symbols of glaucoma, multiple measurements like vertical cup to disc ratio (CDR) in addition to disc width are examined and analysed to identify glaucoma.

CDR is a major concern for clinicians among the clinical features of the glaucoma diagnosis. However, clinical testing by hand-labeling the cup and disc of each image takes time, as is the automatic separation of disk and cup into fundus images.

If you disagree with the separation of disc and cup, you can extract the retinal image of interest (ROI), which provides the first little image that takes very little time to evaluate. The ROI picture is utilised like an intake to Convolutional neural network in this article.

The illness trend in DFIs for glaucoma diagnosis is complicated and subtle, unlike natural pictures. The work of assessing natural sceneries is connected to identifying locations with exceptional look (e.g., texture, shape or color). Glaucoma abnormalities, on the other hand, is only recognised through information and the tester.

DL is a contemporary scientific study that investigates biassed data representation. DL structures are created by merging many linear-indirect data conversions in order to create more ambiguous and, eventually, more helpful presentations. Convolutional neural networks, deep learning structures, are subsequently being utilised successfully to identify pictures and programme applications. To be competitive, DL structures are an extension of multilayer neural (NN) networks, which includes a variety of design and training processes. Spatial consistency, sequence learning, and robustness are examples of these methods. The major focus of this study is to accurately capture the deepest aspects of glaucoma using deep CNN.

2. Literature Review

Glaucoma is illustrated by a lack of optic nerve fibres and cells of brain. This loss may be measured using the size of the central nervous system rim and the optic cup relative to the optic disc. Much of the published research focuses on optical nerve head quality testing employing fundus imaging.

Wong et al., for example, presented a standard technique for computing CDR afterwards receiving an optic cup and an optic disc mask. They evaluated this method on 104 photos and discovered that it generated varied results in fundamental facts by up to 0.2 CDR units.

Cheng et al. presented alternate optic disc and optical cup segmentation method based on a CDR testing system for big pixels. In the two databases, they found areas below the 0.800 and 0.822 curves using their method in 650 images.

We created and trained CNN's six-layer structure from scratch to automatically differentiate glaucomatous fundus images: four conv layers and two completely integrated layers. We performed experiments in two secret repositories, ORIGA-(light) with 650 photos and SCES with 1676 images, and

*Corresponding author: utkarsh.sharma.cs.2018@miet.ac.in

obtained A8 0.831 and 0.887 AUCs, correspondingly. On the ORIGA website, researchers trained the CNN design alongside picking 99 random photos and examining the other 551 images [16]. They trained using 650 photographs from the ORIGA website and tested with all 1676 photos from the SCES website. The ORIGA website has 168 glaucoma photos and 482 common fundus pictures, but the SCES website has 1676 fundus images, with 46 of glaucomatous.

The major consequence is data inequality. Another downside of this research is that acquired results are onerous to repeat since the ORIGA and SCES dataset aren't openly available.

3. Proposed Methodology

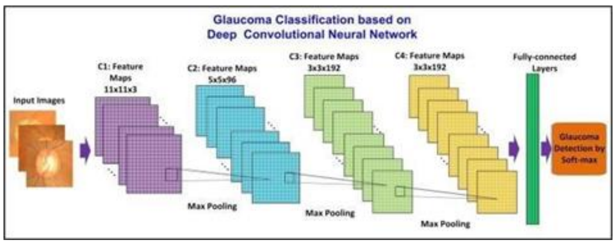

Fig. 1. Systematic review of proposed convolutional neural network-based glaucoma diagnosis. The suggested DL structure is made up of six distinct sections: four flexible layers and two completely linked layers

CNN is the foundation of the deep learning framework proposed for the project. CNN's network contains six layers, as illustrated in Figure 1. The first four are convolutional, while latter two are fully linked. The turnout of the fully linked end layer is introduced into high-grade tissue machine to detect glaucoma. In our suggested reading structure, response-standard layers as well using overlapping layers.

These are frequently utilized to help train tiny features based on random picture samples. The attribute inside picture on that place conceivably blended through adjusting the feature detector and image at the same time. Assume H (n1) and H(n) are the input and output for CNN'S nth layer. Set H(0) to be a duplicate of 2D input picture and H(N) as final N layer output . Allow M(n)1*M(n)I and M(n)O * MO as size of the input and output maps in layer n, respectively. The nth layer's input and output maps are

represented by Q1 and Q0, respectively. The intake of n-th layer will be result from (n-1)th layer, Q n = Q n1 and M n =1 0 1, M n1 . Let H n represent the j- th output-element-map with 0 j. n-th layer, which indeed maps output element for the (n-1)-th layer, $H^{(n1)}$ i-th input-layout-map layout n. Conclusively, the outcome can be found as [8]:

$$Hn = f(SiHi(n-1) * wij(n) + bj(n)1MO(n))$$

Where wij(n) is the kernel that connects the i-th incoming maps to its j-th throughput map.

A. Overlapping-pooling Layers

On CNN, merging layers summarize feature statistics in the image area. The composite layer is composed with a grid of constituent parts isolated by p pixels, all of which reduces the size of the region centred on the merging unit. We find the local integration of the area where p = s. If p s, we have a scattering, which can help with overfilling. As shown in Fig.1, the mass consolidation layers follow both the response setting layers and the conversion layer in our learning structure.

B. CNN-Based Glaucoma Categorization

The result of last two completely integrated layers is inserted in the soft-max classifier to predict magnitude of glaucoma, as illustrated in Fig. 1.

1) Region of Interest (ROI) Extraction

We employed ROI picture like an intrinsic element of CNN in our study, that yields the first compact image which takes less time to analyse than disassembling a disc and a cup [5]. The retinal fundus picture is segmented into groups in the manner of the preceding ARGALI, and the ROI wherein the optic nerve head is situated is resolute by picking grid with the highest probability. Because precise ROI detects the acceleration process and increases glaucoma detection performance, we utilise the approach for effectively distinguishing the ROI in retinal fundus picture. This approach now includes a front processing step to minimize or remove the shiny edge, including the core area of cutting circular and trim radius. After the ROI was released, the output result was reduced to a sample with a static quality of 256 * 256 [19]. Lastly, to minimize the influence of light change on all photos, the mean to all pixels in a disc image is retrieved from each pixel.

2) Cessation and Data Add-Ons

To counteract picture saturation, folks employ data augmentation to avoid unnecessarily expanding the database by changing label storage and stopping model compilation.

Cessation: We employ a pause between two completely integrated layers in our suggested in-depth investigation. To stop, flip the result to every concealed neuron to zero, which can be 0.5. Neurons in CNN that are impaired doesn't participate to advancement and doesn't engage with backward transmission. While testing, we employ every neuron, apart we amplify their effects by 0.5.

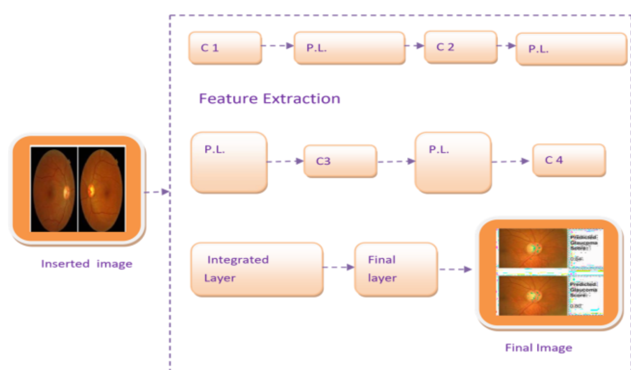

Fig. 2. Structural diagram for predicting glaucoma using CNN algorithm

Data Add-ons: Our network will incur significant overload if we do not use data growth. Image translation and horizontal display are performed as part of the data extension. Data augmentation is accomplished during training by dragging 224 * 224 random packs on 256 * 256 pictures, encompassing their horizontal displays, while coaching our networks on such handouts. During the experiment, CNN forecasts its release of five 224 * 224 leaflets, comprising four corner parts as well as a centre area, along with their lateral visibility and a predictor of the network's soft layer on these ten leaflets. This test approach will be referred to as a multi-view test (MVT).

4. Result and Discussion

We evaluated the glaucoma diagnostic function of the proposed approach using image data sets from glaucoma fundus, ORIGA, SCES.

A. Evaluation Criteria

Here, designers employ lower extremity (AUC) receiver operation characteristic curve (ROC) to assess glaucoma detection efficacy. Curve represents the tradeoff between TPR sensitivity (positive positive rating) and TNR specificity (negative positive rating), which is stated as $TPR = TP / (TP + FN)$, $TNR = TN / (TN + FP)$ where TP and TN represent the count of direct plus indirect negative components, besides FP and FN represent negative and positive values, correspondingly.

B. Experimental Setup

In order to make comparisons, we use the same diagnostic criteria used to diagnose glaucoma in this work. The ORIGA database with clinical glaucoma diagnosis contains 482 general fundus images and 168 glaucoma images. The SCES collection includes 1676 images of fundus, 46 of which are glaucoma patients.

C. Experimental Results

We contrast CNN's conjecture with the latest reconstruction approach to confirm the worth of our CNN in the diagnosis of glaucoma. In the ORIGA database, we utilise the same configuration. The training set comprises of 99 photographs chosen at random from a total of 600 pictures, with the remaining 501 pictures utilised for verification. We utilise 600 photos from ORIGA for mentoring and all 1676 pictures from SCES for test execution. Our AUC technique has values of 0.831 and 0.887 in ORIGA and SCES, respectively. And for advanced reconstructing approach, the AUC standards are 0.823, 0.860 respectively.

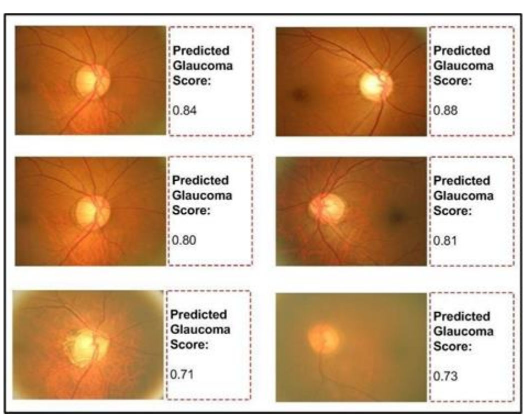

Fig. 3. Suggested glaucoma detection method was used to get the sample diagnosis. Each picture of the fundus is obtained by doctors and the predictable labelling that our system allows.

Figure 3 also provides six model result from this suggested strategy. Doctors diagnose every picture of the fundus, and our system predicts potential labels. In addition to the low image quality in the third line, our method of diagnosing glaucoma, which shows its intensity and durability.

5. Conclusion

Under this paper, we give an overall CNL-based DL architecture towards glaucoma diagnosis that can obtain the discriminating characteristics that help detect the correlations associated with glaucoma. The chosen DL structural design includes six layers: Four convolution layers and two fully linked layers. To prevent over population, we employ conventional response layers and aggregate layers. To boost performance, the drop-off and data-adding techniques are used to the proposed deep CNN. We want to apply our study on CNN-based DL characteristics to identify various eye disorders in the future.

References

[1] Donald L. Budenz, MD, MPH Professor of Ophthalmology, Epidemiology, “Global Perspectives on African Glaucoma African Glaucoma Summit Accra”, August 2010.

[2] M. K. Nath, S. Dandapat, “Techniques of Glaucoma Detection from Colour Fundus Images: A Review”, I. J. Image, Graphics and Signal Processing, 2012, 9, 44-51.

[3] Jack J. Kanski, “Clinical Ophthalmology: systematic Approach,” Seventh edition.

[4] S. Kavitha, S. Karthikeyan, K. Duraiswamy “Neuroretinal Rim Quantification in retinal images to detect glaucoma,” IJCSNS, Vol. 10, No.6, June 2010,

[5] J. Nayak & R. Acharya U, P. S. Bhat, N. Shetty, T C. Lim, “Automated Diagnosis of Glaucoma Using Digital Fundus images”, vol33, pp. 337–346, July 2008.

[6] S. Kavitha, S. Karthikeyan, K. Duraiswamy, “Early Detection of Glaucoma in Retinal Images Using Cup to Disc Ratio”, Second International conference on Computing, Communication and Networking Technologies 2010

[7] T. R. Ganesh Babu, S. Shenbagadevi, “Automatic Detection of Glaucoma Using Fundus Image”, European Journal of Scientific Research, Vol.59 No.1 2011, pp.22- 32.

[8] X. Yang, P. Morrow, B. Scotney, “Optic Nerve Head Segmentation in HRT Images”, School of Computing and Information, Engineering, University of Ulster, 2012.

[9] K. Narasimhan, K. Vijayarekha, K. A. Jogi Narayana, P. Siva Prasad and V. Satish Kumar, “Glaucoma Detection from Fundus Image Using Opencv”, Research Journal of Applied Sciences, Engineering and Technology, 2012.

[10] H. Li, O. Chutatape, “Automated Feature Extraction in Color Retinal Images by a Model Based Approach”, IEEE transactions on biomedical engineering, vol. 51, no. 2, February 2004.

[11] K. Narasimhan, K. Vijayarekha, “An efficient automated system for glaucoma detection using fundus image”, Journal of theoretical and applied information technology, vol. 33 no. 1. November 2011.

[12] U. Rajendra Acharya, Sumeet Dua, Xian Du, Vinitha Sree S, and Chua Kuang Chua, “Automated Diagnoses of Glaucoma using Texture and Higher Order Spectra Features.” IEEE Transaction on information technology biomedical vol. 15, no. 3, May 2011.

[13] James Lowell, Andrew Hunter, David Steel, Ansu Basu, Robert Ryder, Eric Fletcher, and Lee Kennedy,’’ Optic Nerve Head Segmentation’’, IEEE Transactions on medical imaging, vol. 23, no. 2, february 2004.

[14] Aliaa Abdel-Haleim Abdel-Razik Youssif, Atef Zaki Ghalwash, and Amr Ahmed Sabry Abdel-Rahman Ghoneim, “Optic Disc Detection from Normalized Digital Fundus Images by Means of a Vessels’ Direction Matched Filter”, IEEE Transactions on medical imaging, vol. 27, no. 1, january 2008.

[15] Juan Xu, Opas Chutatape, Eric Sungc, Ce Zheng, Paul Chew Tec Kuan, “Optic disk feature extraction via modified deformable model technique

for glaucoma analysis", The journal of pattern recognition society, October 2006.

[16] Bazán, I. and Ramírez-García, A., 2019, September. Two methods for computer simulated Glaucoma Diagnosis A-Scan signals. In 2019 16th International Conference on Electrical Engineering, Computing Science and Automatic Control (CCE) (pp. 1-5) IEEE.

[17] Li P., Geng, L., Zhu, W., Shi, F. and Chen, X., 2020, April. Automatic angles closure screening Glaucoma Based on Scleral track location in the prior OCT segment. In 2020 IEEE 17th International Symposium on Biomedical Imaging (ISBI) (pp. 1387-1390) IEEE.

[18] Ovreiu, S., Cristescu, I., Balta, F., Sultana, A. And Ovreiu, E., 2020, June. Residual networks early warning of glaucoma. In 2020 13th International Conference on Communications (COMM) (pp. 161-164). IEEE.

[19] Palakvangsa-Na-Ayudhya, S., Sapthamrong, T., Sunthornwutthikrai, K. and Sakiyalak, D., 2020, June. Glauco VIZ: R-CNN Mask Recognition Assistance System for Early Glaucoma. In 2020 17th International Conference on Electrical Engineering/Electronics, Computer, Telecommunications and Information Technology (ECTI- CON) (pp. 364- 367). IEEE.

[20] Naseer Bajwa, M., Singh, G. A. P., Neumeier, W., Malik, M. I., Dengel, A. and Ahmed, S., 2020. G1020: A Benchmark Image Dataset for the Identification of Machine Helped Glaucoma, 2006.